Climate Zones for Maritime Clouds

A. B. White and D. Ruffieux
Cooperative Institute for Research in Environmental Sciences
University of Colorado at Boulder/National Oceanic and Atmospheric Administration
Boulder, Colorado

C. W. Fairall
National Oceanic and Atmospheric Administration
Environmental Research Laboratories
Environmental Technology Laboratory
Boulder, Colorado

Introduction

In this paper we use a commercially available lidar ceilometer to investigate how the basic structure of marine boundary-layer clouds varies for four different marine climate regimes. We obtained most of the data used in this analysis from ship-based ceilometer measurements recorded during several different atmospheric and oceanographic field programs conducted in the Atlantic and Pacific oceans. For comparison, we show the results obtained at a mid-latitude continental location and at an ice camp on the Arctic ice shelf. For each analyzed case, we use an extended time series to generate meaningful cloud base and cloud fraction statistics.

The Vaisala CT 12K ceilometer uses a GaAs diode laser to produce short (150 ns), high-intensity pulses of infrared radiation (904 nm wavelength). The return signals from a large number of consecutive pulses are coherently summed to boost the signal-to-noise ratio. Each resulting 30-s profile of backscattered power (15-m resolution) is analyzed to detect cloud layers using a specified cloud detection limit. In addition to measurements of cloud base, the ceilometer can also provide information on cloud fraction using a time series of the "cloud" or "no cloud" status reported in the 30-s data. Additional details on operation of the CT 12K are given by Schubert et al. (1987).

Data Interpretation and Limitations

Users of ceilometer data must be aware of several key points. First, because the maximum vertical range of the CT 12K is 3480 m, cirrus and other mid- to high-level clouds cannot be detected. Second, the lidar beam of the CT 12K points vertically. Therefore, depending on the horizontal distribution of clouds, the overhead, time-averaged cloud fraction deduced from the ceilometer may be much different statistically than the area-averaged cloud fraction obtained from satellite measurements. Third, the cloud base determined by the ceilometer may differ from the base that is humanly visible or that can be measured by different instruments such as millimeter wavelength radars. Fourth, for a cloud that tilts in the presence of wind shear, the ceilometer will actually report the height of the side of the cloud as it passes over the instrument. Finally, there are instances when the ceilometer determines the sky condition to be fully obscured, but no cloud base can be detected. These situations occur at low- and mid-latitudes in fog or precipitation, cases that naturally should be included in a computation of cloud fraction. However, at higher latitudes, additional meteorological conditions such as blowing snow and "diamond dust" (ice particles) can occur with appreciable frequency. Although

it is not clear how to handle these particular phenomena, for consistency, we included the fully obscured, without-cloud-base points in our computation of cloud fractions for the one high-latitude case we examined.

Results

The ceilometer data are presented in two formats. Summary statistics, along with the names, dates, locations, and cloud types observed for each of the field programs, are given in Table 1. Diurnally averaged cloud fraction and cloud base statistics, as well as cloud base frequency distributions, are shown graphically in Figure 1.

The four marine cases are organized in the order shown in Table 1 to provide a logical transition from the mid-latitude, stratocumulus-topped marine boundary layer to the tropical, convective marine boundary layer. Data from the First ISCCP[a] Regional Experiment (FIRE) and the San Clemente Ocean Probing Experiment (SCOPE) were combined because of the proximity of the experiment locations and because it allowed us to better match the number of 30-s profiles observed in the other field programs. This composite was also sensible because of the similarities we observed in the statistics generated for the two individual data sets.

The cloud fraction and cloud base statistics exhibit both expected and unexpected behavior. For example, in Figure 1, the diurnally averaged cloud fraction curves for FIRE/SCOPE and the Atlantic Stratocumulus Transition EXperiment (ASTEX) show marked similarities during the daytime, but differ for at least part of the night. The decrease in cloud fraction from mid-morning to early afternoon observed for these two cases is consistent with the theory of boundary-layer decoupling reviewed by Driedonks and Duynkerke (1989). Reconnection of the cloud layer with the subcloud layer may explain the increase in cloud fraction that starts near 1430 and persists until after sunset. The Arctic Leads Experiment (LEADEX) also exhibits a somewhat surprising and, as yet, unexplained diurnal variation in cloud fraction. It is also interesting to note that although deep convection and rainfall were observed much more frequently during the Coupled Ocean-Atmosphere Response Experiment (COARE) than during

the Tropical Instability Wave Experiment (TIWE), the average boundary layer cloud fraction for TIWE is slightly higher than for COARE (see Table 1).

The only site with a notable diurnal variation in cloud base is the Boulder Atmospheric Observatory (BAO). The increase in cloud base during the afternoon and early evening occurs at the same time that thunderstorms form on the plains just east of the Rocky Mountains in Colorado. The large difference between the average stratocumulus bases observed during FIRE/SCOPE and ASTEX may be due to a combination of factors, including distance from the coastline, sea surface temperature, and average strength of subsidence above the marine boundary layer.

Perhaps most descriptive are the cloud base frequency distributions. The FIRE/SCOPE distribution is made up almost completely of stratocumulus and has the narrowest width and the lowest median value of all the distributions. The TIWE and COARE distributions are composed of two distinct parts. The lower part has a well-defined peak between 500 m and 900 m that corresponds to trade cumulus forming near the lifting condensation level. Keeping in mind that the ceilometer also sees the heights of the sides of thick clouds, the tail of these distributions (i.e., the part from 1 to 4 km) indicates deeper convection. The ASTEX distribution is unlike the other three marine cases. The region from 500 m to 800 m is where the so-called scud clouds form in the decoupled boundary layer. The distribution above 800 m is due to variations in the height of the stratus layer. Low clouds and diamond dust occupy roughly the lowest 500 m of the LEADEX distribution. The tail of this distribution is presumably due to clouds associated with passing weather systems. The widest distribution is from BAO, where summertime convection and nearby topography combine to produce a variety of clouds.

Summary

We used ceilometer measurements to calculate bulk cloud properties for various climate zones. We do not propose that the length of record for any of the data sets we used is sufficient to define a cloud climatology for the analyzed regions. We do hope, however, that these measurements

---

(a) International Satellite Cloud Climatology Project.

Table 1. Cloud statistics generated from extended time series of ceilometer data.

Experiment Name	Dates	Location Latitude (deg) Longitude (deg)	Total Number of 30-s Profiles	Cloud Fraction	Cloud Base (m)			Primary Cloud Types
					20th percentile	50th percentile	80th percentile	
FIRE (First International Satellite Cloud Climatology Program Regional Experiment)	July 1987	San Nicolas Island Eastern Pacific 33 N 120 W						
SCOPE (San Clemente Ocean Probing Experiment)	Sept 1993	R/V *Titan* Eastern Pacific 33 N 118 W	8.05×10^5	0.69	300	457	750	Marine Stratus
TIWE (Tropical Instability Wave Experiment)	Nov-Dec 1991	R/V *Moana Wave* Equatorial Pacific 0 140 W	5.68×10^5	0.26	625	945	1585	Trade Cumulus
ASTEX (Atlantic Stratocumulus Transition Experiment)	June 1992	R/V *Malcolm Baldridge* Eastern Atlantic 27-37 N 22-27 W	5.81×10^5	0.45	594	1021	1463	Marine Stratus Trade Cumulus
COARE (Coupled Ocean-Atmosphere Response Experiment)	Nov 1992-Feb 1993	R/V *Moana Wave* Western Pacific 2 S-5 N 153-157 E	1.26×10^6	0.22	686	1052	1844	Trade Cumulus (suppressed) ... Cumulonimbus (convective)
BAO (Boulder Atmospheric Observatory)	July-Sept 1993	Erie, Colorado 40 N 105 W	1.45×10^6	0.18	472	1478	3002	Cumulus ... Cumulonimbus
LEADEX (Arctic Leads Experiment)	March-Apr 1992	Arctic Ice Camp 73 N 145 N	6.21×10^5	0.40	168	655	1661	Arctic Stratus

will be useful to those involved in the planning of future field work. The compact size, durability, and ease of operation make the ceilometer a strong candidate for inclusion in any cloud-observing experiment.

Acknowledgments

References

Driedonks, A.G.M., and P. G. Duynkerke. 1989. Current problems in the stratocumulus-topped atmospheric boundary layer. *Bound.-Layer Meteor.* **46**:275-304.

Schubert, W. H., S. K. Cox, P. E. Ciesielski, and C. M. Johnson-Pasqua. 1987. Operation of a ceilometer during the FIRE Marine Stratocumulus Experiment. Dept. of Atmos. Science Paper No. 420, Colorado State University, Fort Collins, Colorado.
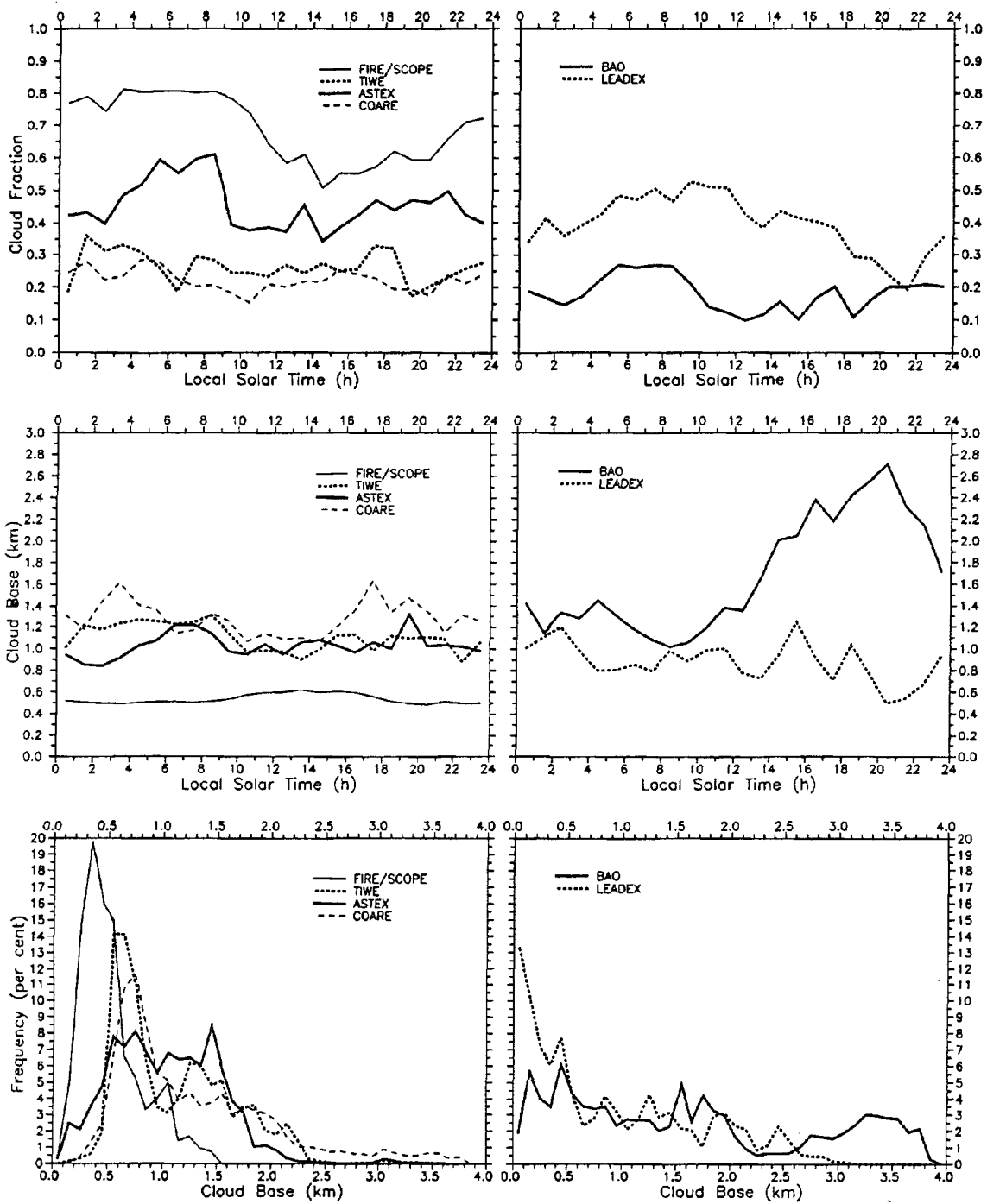
Figure 1. Diurnally averaged cloud fraction (top panels), cloud base (middle panels), and cloud base frequency distribution (bottom panels) calculated from extended time series of ceilometer data.